
MMbeddings: Parameter-Efficient, Low-Overfitting Probabilistic Embeddings Inspired by Nonlinear Mixed Models

Giora Simchoni

Department of Statistics

Tel Aviv University

Tel Aviv, Israel, 69978

gsimchoni@tauex.tau.ac.il

Saharon Rosset

Department of Statistics

Tel Aviv University

Tel Aviv, Israel, 69978

saharon@tauex.tau.ac.il

Abstract

We present MMbeddings, a probabilistic embedding approach that reinterprets categorical embeddings through the lens of nonlinear mixed models, effectively bridging classical statistical theory with modern deep learning. By treating embeddings as latent random effects within a variational autoencoder framework, our method substantially decreases the number of parameters—from the conventional embedding approach of cardinality \times embedding dimension, which quickly becomes infeasible with large cardinalities, to a significantly smaller, cardinality-independent number determined primarily by the encoder architecture. This reduction dramatically mitigates overfitting and computational burden in high-cardinality settings. Extensive experiments on simulated and real datasets, encompassing collaborative filtering and tabular regression tasks using varied architectures, demonstrate that MMbeddings consistently outperforms traditional embeddings, underscoring its potential across diverse machine learning applications.

1 Introduction

Categorical features play a critical role in a variety of predictive modeling tasks, yet efficiently managing these features becomes increasingly challenging as their cardinality grows [28]. For instance, collaborative filtering methods commonly deal with categorical features such as user and item identifiers, each with cardinality in the thousands or even millions, resulting in extremely high-dimensional representations and posing substantial computational and statistical challenges [see, e.g., 9]. One-hot encoding (OHE) represents each category of a categorical feature of q levels as a separate binary indicator feature, leading to q additional features. When cardinality is high, this approach results in a computationally burdensome and inefficient representation that fails to encode similarity between related categories and significantly increases the risk of overfitting [8].

Entity embeddings represent categorical features by mapping each of the q distinct categories into a continuous d -dimensional vector space using a learned embedding matrix $\mathbf{B} \in \mathbb{R}^{q \times d}$ [5, 6]. The embeddings approach has become a ubiquitous modeling strategy, significantly improving performance over traditional encodings, with applications ranging from tabular and relational data in predictive modeling tasks [16] to representing tokens in natural language processing [19] and powering recent state-of-the-art architectures such as transformers [11]. While this representation captures semantic relationships between categories and substantially reduces dimensionality compared to OHE, it could still introduce a considerable number of parameters, leading to high computational complexity and vulnerability to overfitting [4].

Although embedding layers seem like a modern machine learning innovation, categorical data embeddings have quietly existed within statistical models for decades, rooted implicitly through the

use of random effects in linear and non-linear mixed models [18]. Linear mixed models (LMM) distinguish between fixed effects (FE) – standard model parameters estimated directly from data – and random effects (RE), which are treated as random variables whose distributions are estimated instead. This distinction effectively handles high-cardinality categorical features or clustering structures within data [29]. For example, in medical research, treatment type (a carefully designed experimental condition) is modeled as a FE, while observational categorical features such as a patient’s city – with potentially thousands of unique levels – are modeled as RE, typically assumed to follow a normal distribution with mean zero and unknown variance. Extending this idea, non-linear mixed models (NLMM) with d -dimensional RE assigned to each categorical unit can be viewed as representing these categories through latent embeddings drawn from probability distributions, thus offering a robust and theoretically grounded probabilistic interpretation of embeddings. This connection will be elaborated in Section 2.

Building upon this historical connection between embeddings and NLMM, we introduce MMembeddings – named to explicitly highlight their foundation in “mixed models embeddings.” Our proposed approach leverages a novel variational autoencoder (VAE) architecture, explicitly modeling embeddings as RE within a VAE framework while minimizing a negative log-likelihood (NLL) loss. By treating embeddings as latent variables drawn from probability distributions, this architecture naturally imposes regularization, substantially reduces the number of parameters, and mitigates overfitting. Extensive experiments on both simulated datasets and real-world data demonstrate that MMembeddings achieve superior predictive performance, consistently outperforming traditional entity embeddings and standard encoding techniques across metrics such as MSE in regression and AUC in classification.

The remainder of this paper is structured as follows. Section 2 reviews background concepts and discusses related methods in entity embeddings and mixed models. In Section 3, we formally introduce our proposed method, MMembeddings, detailing its variational architecture and probabilistic mechanism. Extensive experiments demonstrating the effectiveness of MMembeddings compared to alternative methods, are presented in Section 4. Finally, Section 5 summarizes our contributions and suggests potential directions for future research.

2 Background and related methods

NLMM have a rich history in statistical modeling, with the landmark paper by Lindstrom and Bates [17] introducing NLMM specifically for analyzing repeated measures data. One illustrative example from their seminal work involved repeated circumference measurements (x_{ij}, y_{ij}) of orange trees, where x_{ij} denotes the time of the i -th measurement for tree j ($j = 1, \dots, q$ trees, $i = 1, \dots, n_j$ measurements per tree). Lindstrom and Bates proposed the logistic NLMM:

$$y_{ij} = \frac{\beta_1 + b_{1j}}{1 + \exp\left(-\frac{x_{ij} - (\beta_2 + b_{2j})}{\beta_3 + b_{3j}}\right)} + \varepsilon_{ij}, \quad (1)$$

where $\beta_1, \beta_2, \beta_3$ represent FE and ε_{ij} random Gaussian noise. Specifically, β_1 describes the average asymptotic circumference of the tree, β_2 indicates the average time a tree reaches half its maximum circumference, and β_3 acts as a scale parameter. Additionally, each tree j has associated RE $b_{kj} \sim \mathcal{N}(0, \sigma_{b_k}^2)$ for $k = 1, 2, 3$, where $\sigma_{b_k}^2$ are variance components estimated from data. Notably, these RE can be stacked into a matrix $\mathbf{B}_{q \times 3}$, mapping each tree to a continuous latent embedding in a $d = 3$ dimensional space, closely aligning with the modern concept of embeddings. Lindstrom and Bates devised a two-step iterative maximum likelihood procedure: initially estimating FE and RE given initial variance components, then refining variance estimates using a Newton-Raphson approach to maximize the conditional log-likelihood of $y|\mathbf{B}$. However, their method was developed in a relatively “small data” context (their original dataset contained only $q = 5$ trees, each measured $n_j = 7$ times), limiting scalability. Furthermore, their approach required explicitly specifying a parametric non-linear function. Our proposed method builds upon this foundational work, generalizing Lindstrom and Bates’ model to handle large-scale data. Instead of explicitly defining a parametric relationship, we employ a deep neural network (DNN) within an encoder-decoder architecture to flexibly model complex, non-linear relationships. By minimizing a variational loss that serves as an upper bound to the NLL, our approach effectively unifies and modernizes Lindstrom and Bates’ two-step iterative procedure, leveraging contemporary machine learning practices such as mini-batch processing and stochastic gradient descent (SGD).

Several recent approaches have attempted to integrate RE into DNN, with no specific focus on embeddings. MeNets [37] focus on random intercept models, specifically modeling a single categorical feature with a single RE, represented as $y_{ij} = f(\mathbf{x}_{ij}) + b_{0j} + \varepsilon_{ij}$, where $b_{0j} \sim \mathcal{N}(0, \sigma_b^2)$. Other methods like sgGP [3] and deep kernel learning [33, 34] integrate Gaussian processes into deep learning frameworks, particularly tailored to spatial datasets with measurements at q distinct locations. LMMNN [29] incorporates RE into DNN by decomposing inputs into separate FE features \mathbf{x}_{ij} and RE features \mathbf{z}_{ij} , using a LMM-inspired formulation $y_{ij} = f(\mathbf{x}_{ij}) + g(\mathbf{z}_{ij})\mathbf{b}_j + \varepsilon_{ij}$, with Gaussian NLL loss. However, this strict separation limits identifiability when attempting to represent each categorical unit j with a d -dimensional RE vector \mathbf{b}_j (with $d > 1$), due to inherent identifiability issues highlighted in Lavielle and Aarons [14]. A recent approach closely related to ours, which we term REembeddings [24], explicitly models embeddings as RE within an NLMM, minimizing a variational bound on the NLL. However, REembeddings parameterize embeddings using two separate embedding layers – one each for the means and log-variances for all elements in $\mathbf{B}_{q \times d}$ – resulting in a prohibitive number of parameters ($2Kqd$ parameters for K categorical features of cardinality q with embedding dimension d). In contrast, our proposed method leverages a neural encoder to output only d means and log-variances to produce posterior distributions for embeddings based on input features \mathbf{X} and outcomes \mathbf{y} , requiring only $M + 2d$ parameters (where M is the number of encoder parameters, typically much smaller than Kqd). Our method significantly reduces overfitting risks with improved predictive performance as demonstrated in Section 4.

Several alternative encoding techniques generate categorical embeddings without explicit training, such as feature hashing [32], mean-encoding [13], and PCA-encoding [15]. Although computationally efficient, these heuristic methods typically yield inferior predictive performance compared to learned embeddings, as demonstrated in our experiments in Section 4.

A distinct branch of research has aimed to curtail the growing complexity and dimensionality of trainable embeddings. Hash Embeddings [31] employ feature hashing within embedding layers to substantially decrease the parameter count, mitigating collisions through multiple hash functions and learned combinations. Similarly, Compositional Embeddings [27] represent categories through combinations of shared sub-embeddings, significantly reducing the number of embedding parameters needed. Most notably, Unified Embeddings (UEmbeddings) [4] generalize these ideas by using a unified embedding framework that blends hashing and compositional techniques, mapping categories from different features into a shared latent space through a single embedding matrix $\mathbf{B}_{qu \times d}$. While these methods effectively reduce parameter counts, they tend to be predominantly architecture-driven, relying on heuristic design choices without explicit underlying probabilistic or statistical models.

Recent years have witnessed considerable progress in advanced methods tailored to tabular data, particularly emphasizing categorical feature representations through embedding layers. Factorization machines [23] and their DNN variant, DeepFM [7], explicitly model feature interactions leveraging embeddings. Similarly, collaborative filtering methods [26] and their DNN extension, Neural Collaborative Filtering [9], combine embeddings to capture complex user-item interactions. More recently, TabNet [1] introduced attention mechanisms to sequentially focus on relevant features, while TabTransformer [11] applies transformer architectures specifically to categorical data embeddings, effectively modeling interactions among categories. Principally, despite their methodological diversity, these sophisticated approaches uniformly rely on standard embedding layers. In Section 4, we directly compare some of these methods equipped with conventional embeddings against our proposed MMembeddings framework.

3 Proposed method: MMembeddings

Consider an observation $y_{ij} \in \mathbb{R}$, representing the i -th data point within the j -th level of a single categorical feature that has q distinct levels (with $j = 1, \dots, q$ and $i = 1, \dots, n_j$). Extending the formulation given in (1), our model can be expressed more generally as:

$$y_{ij} = f(\mathbf{x}_{ij}, \mathbf{b}_j) + \varepsilon_{ij}, \quad (2)$$

where $\mathbf{x}_{ij} \in \mathbb{R}^p$ denotes the vector of additional features, $\varepsilon_{ij} \sim \mathcal{N}(0, \sigma^2)$ is Gaussian noise, f is a non-linear function typically modeled with DNN, and $\mathbf{b}_j \in \mathbb{R}^d$ is the RE vector, which we refer to as MMembeddings. Typically, \mathbf{b}_j is assumed to follow a multivariate normal distribution $\mathcal{N}(\mathbf{0}, \mathbf{D})$, with \mathbf{D} being a general covariance matrix. However, it often proves beneficial to assume \mathbf{D} is diagonal, implying each element b_{mj} of \mathbf{b}_j independently follows $\mathcal{N}(0, \sigma_m^2)$, $m = 1, \dots, d$.

To accommodate multiple categorical features, we expand our notation. For instance, with two categorical features, the observation can be written as $f(\mathbf{x}_{ijl}, \mathbf{b}_j, \mathbf{b}_l)$, reflecting the inclusion of two MMembeddings vectors corresponding to each categorical feature. Generalizing further, for K categorical features, each with cardinality q_k , we collect the corresponding MMembeddings vectors into $q_k \times d_k$ embedding matrices \mathbf{B}_k . Consequently, we succinctly represent our model in vectorized form:

$$\mathbf{y} = f(\mathbf{X}, \mathbf{B}_1, \dots, \mathbf{B}_K) + \boldsymbol{\varepsilon}, \quad (3)$$

where $\mathbf{y} \in \mathbb{R}^n$ is the response vector, \mathbf{X} is the $n \times p$ matrix of covariates, and $\boldsymbol{\varepsilon} \in \mathbb{R}^n$ is a Gaussian noise vector.

Consider again the scenario with a single categorical feature described in (2), and denote the vector of observations within cluster j as $\mathbf{y}_j = [y_{1j}, \dots, y_{nj,j}]$. Directly computing the marginal log-likelihood of \mathbf{y}_j , obtained by integrating out the MMembeddings \mathbf{b}_j – specifically, $\log p(\mathbf{y}_j) = \log \int p(\mathbf{y}_j | \mathbf{b}_j) p(\mathbf{b}_j) d\mathbf{b}_j$ – is computationally intractable. A standard solution from variational Bayes [see, e.g., 12] introduces an approximating distribution $q(\mathbf{b}_j | \mathbf{y}_j)$ for the posterior of \mathbf{b}_j . This approximation yields the evidence lower bound (ELBO), providing a tractable lower bound to the log-likelihood:

$$\log p(\mathbf{y}_j) \geq \text{ELBO} := \mathbb{E}_q [\log p(\mathbf{y}_j | \mathbf{b}_j)] - D_{KL} [q(\mathbf{b}_j | \mathbf{y}_j) \| p(\mathbf{b}_j)]. \quad (4)$$

Maximizing the ELBO thus corresponds to simultaneously maximizing the expected conditional log-likelihood $\mathbb{E}_q [\log p(\mathbf{y}_j | \mathbf{b}_j)]$ and minimizing the Kullback–Leibler divergence between the approximate posterior $q(\mathbf{b}_j | \mathbf{y}_j)$ and the prior distribution $p(\mathbf{b}_j)$. The conditional distribution $p(\mathbf{y}_j | \mathbf{b}_j)$ is Gaussian $\mathcal{N}(f(\mathbf{x}_j, \mathbf{b}_j), \sigma^2 \mathbf{I}_{n_j})$ as indicated by (2). In practice, a single sample drawn from $q(\mathbf{b}_j | \mathbf{y}_j)$ is typically sufficient to estimate the expectation. Moreover, following the mean-field variational inference framework, we assume $q(\mathbf{b}_j | \mathbf{y}_j)$ factorizes over dimensions, i.e., $q(\mathbf{b}_j | \mathbf{y}_j) = \prod_{m=1}^d q_m(b_{mj} | \mathbf{y}_j)$. The distribution of each factor $q_m(b_{mj} | \mathbf{y}_j)$ is assumed Gaussian with variational parameters μ_{mj} and τ_{mj}^2 , that is, $q_m(b_{mj} | \mathbf{y}_j) = \mathcal{N}(\mu_{mj}, \tau_{mj}^2)$. These variational parameters are fitted during training.

Figure 1 illustrates the overall architecture of MMembeddings. As commonly adopted in the VAE framework, we utilize a neural network encoder to parameterize the approximate posterior distribution $q(\mathbf{b}_j | \mathbf{y}_j)$. For each observation (\mathbf{x}_i, y_i) of cluster j , this encoder produces vectors of d means $\boldsymbol{\mu}_j$ and d log-variances $\log \boldsymbol{\tau}_j^2$ for the latent embedding \mathbf{b}_j . Using the reparameterization trick, we sample \mathbf{b}_j from this variational posterior to maintain differentiability during training. A separate neural network decoder then models the nonlinear relationship f , taking as input the sampled embedding \mathbf{b}_j along with the covariates \mathbf{x}_i . The decoder architecture can vary widely – including a simple multilayer perceptron (MLP), neural collaborative filtering, or transformer – as we demonstrate in Section 4. The decoder, crucially, is later employed independently at inference for prediction tasks.

The negative ELBO serves as our training objective. Simplifying this, for an individual observation (\mathbf{x}_i, y_i) from cluster j , the negative ELBO can be explicitly written as:

$$-\text{ELBO}_i = \frac{1}{2} \log(2\pi\sigma^2) + \frac{1}{2\sigma^2} (y_i - f(\mathbf{x}_i, \mathbf{b}_j))^2 + \frac{1}{2} \sum_{m=1}^d \left[-1 - \log \tau_{mj}^2 + \log \sigma_m^2 + \frac{\mu_{mj}^2}{\sigma_m^2} + \frac{\tau_{mj}^2}{\sigma_m^2} \right].$$

When moving to a minibatch ξ of size n_ξ , comprising observations $[(\mathbf{x}_1^\xi, y_1^\xi), \dots, (\mathbf{x}_{n_\xi}^\xi, y_{n_\xi}^\xi)]$, different categorical levels can appear multiple times, once, or not at all. Although we initially sample n_ξ MMembedding vectors $[\mathbf{b}_1^\xi, \dots, \mathbf{b}_i^\xi, \dots, \mathbf{b}_{n_\xi}^\xi]$, each sample corresponds to a specific level j of the categorical feature. To obtain the q MMembedding vectors per categorical level $[\mathbf{b}_1^\xi, \dots, \mathbf{b}_j^\xi, \dots, \mathbf{b}_q^\xi]$, we average all sampled vectors belonging to the same level, setting zeros for any levels absent in the current minibatch. This averaging procedure significantly reduces the number of parameters from $q \times d$ per categorical feature, as employed by methods such as REembeddings, thereby mitigating overfitting risks. It is symbolized by \odot in Figure 1, and is efficiently implemented in a vectorized manner to enhance computational performance. Furthermore, before computing the loss given by (5), we average the encoder outputs $\boldsymbol{\mu}_i^\xi$ and $\log \left([\boldsymbol{\tau}_i^\xi]^2 \right)$ across observations belonging to each

categorical level j :

$$\boldsymbol{\mu}_j^\xi = \frac{1}{n_{\xi j}} \sum_{i \in \text{cluster } j} \boldsymbol{\mu}_i^\xi, \quad \log \left(\left[\boldsymbol{\tau}_j^\xi \right]^2 \right) = \log \left[\frac{1}{n_{\xi j}^2} \sum_{i \in \text{cluster } j} \exp \left(\log \left(\left[\boldsymbol{\tau}_i^\xi \right]^2 \right) \right) \right],$$

where $n_{\xi j}$ denotes the number of observations in cluster j within the minibatch ξ , and $\boldsymbol{\mu}_j^\xi = \mathbf{0}$, $\log \left(\left[\boldsymbol{\tau}_j^\xi \right]^2 \right) = \mathbf{0}$ if no observations from level j are present. While this averaging scheme may appear straightforward, it follows from a careful consideration of alternative strategies, as discussed in Appendix A.

Aggregating over the minibatch ξ , and considering K categorical features each with cardinality q_k and embedding dimension d_k , yields the full negative ELBO loss for MMbeddings:

$$\begin{aligned} -ELBO_\xi(f, q) = & \frac{n_\xi}{2} \log(2\pi\sigma^2) + \frac{1}{2\sigma^2} \sum_{i=1}^{n_\xi} \left(y_i^\xi - f \left(\mathbf{x}_i^\xi, \mathbf{b}_{(*1)}^\xi, \dots, \mathbf{b}_{(*K)}^\xi \right) \right)^2 \\ & + \frac{\beta_V}{2} \sum_{k=1}^K \sum_{j=1}^{q_k} \sum_{m=1}^{d_k} \left[-1 - \log \left(\left[\boldsymbol{\tau}_{mjk}^\xi \right]^2 \right) + \log \sigma_{mk}^2 + \frac{\left(\mu_{mjk}^\xi \right)^2}{\sigma_{mk}^2} + \frac{\left(\boldsymbol{\tau}_{mjk}^\xi \right)^2}{\sigma_{mk}^2} \right], \end{aligned} \quad (5)$$

where $\mathbf{b}_{(*1)}^\xi, \dots, \mathbf{b}_{(*K)}^\xi$ represent the corresponding sampled MMbeddings for each observation in the minibatch, and β_V is a hyperparameter borrowed from the β -VAE literature, which often enhances model performance [10, 25]. Note that the second term in the ELBO aggregates KL divergences over all categories and features, thus reflecting the full dataset, whereas the first term sums only over the minibatch; accordingly, balancing these terms requires scaling, and we empirically observe that setting $\beta_V \approx \frac{n_\xi}{N}$ yields good results. The prior variances σ^2 and σ_{mk}^2 are necessary components of the model and can either be treated as fixed hyperparameters specified a priori, tuned through grid search, or optimized via SGD. In our implementation below, unless stated otherwise, we adopt the simplest prior assumption by fixing all prior variances to 1 during training and subsequently demonstrate the robustness of MMbeddings even when this simplifying assumption does not hold.

Typically, at inference time, our primary interest is in predicting outcomes for new, unseen data after training the encoder and decoder. Suppose $(\mathbf{X}_{tr}, \mathbf{y}_{tr})$ and \mathbf{X}_{te} denote the training and testing datasets, respectively. To reconstruct predictions $\hat{\mathbf{y}}_{te}$, we first use the trained encoder to generate embedding vectors \mathbf{b} for all observations in the training set. These embeddings are grouped by their corresponding categorical levels, resulting in estimated MMembedding matrices $\hat{\mathbf{B}}_k$ of size $q_k \times d_k$ for each categorical feature k . Finally, predictions for the testing data are obtained by applying the trained decoder \hat{f} to \mathbf{X}_{te} together with these embedding matrices, yielding $\hat{\mathbf{y}}_{te} = \hat{f}(\mathbf{X}_{te}, \hat{\mathbf{B}}_1, \dots, \hat{\mathbf{B}}_K)$. In practice, we often found it beneficial to freeze the embedding matrices $\hat{\mathbf{B}}_k$ after initial training and subsequently fine-tune only the decoder for several additional epochs.

4 Experiments

We now present experimental results using both simulated and real datasets to demonstrate the effectiveness of the MMbeddings approach. We begin our analysis with simulated data, designed specifically to capture scenarios involving high-cardinality categorical features. All experiments were conducted using Python in Google Colab with Keras on TensorFlow, and code and data are publicly available at <https://github.com/gsimchoni/mmbbeddings>.

4.1 Simulated data

We generate data according to model (2), where each observation \mathbf{x}_{ij} contains $p = 10$ features sampled uniformly from $\mathcal{U}(-1, 1)$. The embeddings \mathbf{b}_j are $d = 10$ -dimensional vectors drawn from $\mathcal{N}(\mathbf{0}, \mathbf{D})$, with covariance matrix $\mathbf{D} = \sigma_b^2 \mathbf{I}_d$, and variance parameter σ_b^2 fixed on 1, or varied in further experiments in Appendix D. The nonlinear function f , inspired by Lindstrom and Bates,

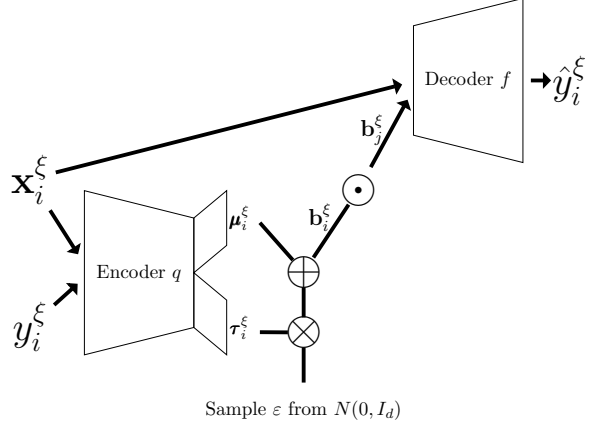


Figure 1: MMembeddings scheme for a single categorical feature, combining an encoder to parameterize the variational posterior $q(\mathbf{b}_j|\mathbf{y}_j)$ and a decoder modeling the nonlinear function $f(\mathbf{x}_{ij}, \mathbf{b}_j)$.

uniquely combines each feature with fixed and random effects from the $\mathbf{B}_{q \times d}$ embeddings and can be viewed in Appendix B.

Additionally, a noise term ε_{ij} is introduced from $\mathcal{N}(0, \sigma^2)$ with $\sigma^2 = 1$, and this $f(\mathbf{X}, \mathbf{B}) + \varepsilon$ is used as \mathbf{y} for regression or binarized for classification. We examine scenarios with increasing cardinality $q \in \{10^2, 10^3, 10^4, 10^5\}$, maintaining $n = 10q$ overall, with varying group sizes n_j , sampled from a multinomial distribution.

We compare MMembeddings against alternative embedding methods, including standard embeddings, L2-regularized embeddings (EmbedL2), REembeddings, UEmbeddings, and a baseline model which is agnostic to the categorical feature (using only the feature matrix \mathbf{X}). Other methods such as mean-encoding, PCA-encoding, feature hashing, LMMNN, TabNet and TabTransformer were also tested but performed badly, and their detailed outcomes are provided in Appendix D. Each method employs a decoder architecture with a two-layer MLP with two layers of 10 neurons each, and ReLU activations. MMembeddings adds an encoder which consists of a two-layer MLP with layer sizes of 100 neurons each, also using ReLU activations. All models were trained using early stopping based on performance on a 10% validation set, with patience set to 10 epochs and batch size equal to q . Training proceeded for a maximum of 1000 epochs. For MMembeddings specifically, the parameter β_V was fixed at 0.001, as the performance was stable across similarly small values. The latent dimension d was treated as known in all cases, with sensitivity analyses of this parameter included in Appendix D.

Each experiment was repeated 10 times, evaluating performance on 100K unseen test observations. For regression tasks, we measured mean squared error MSE_Y ; for classification, we used the area under the ROC curve AUC_Y . Embedding quality was assessed by computing the normalized root mean squared error ($RMSE_D$) between pairwise Euclidean $q \times q$ distances of true embeddings \mathbf{B} and estimated embeddings $\hat{\mathbf{B}}$ (see Appendix C for details). Recognizing the practical significance of embeddings for downstream tasks, we also simulated a binary outcome from a linear model using the true embeddings and reported the resulting AUC_B after fitting logistic regression on the estimated embeddings $\hat{\mathbf{B}}$.

Table 1 shows the performance comparison across embedding methods for simulated regression and classification tasks with varying cardinalities. MMembeddings consistently outperforms alternative methods in predictive performance (MSE_Y and AUC_Y), embedding quality ($RMSE_D$), and downstream utility (AUC_B). Improvements become particularly pronounced with increasing cardinality, underscoring MMembeddings' robustness in handling high-cardinality categorical features. Notably, MMembeddings maintains a fixed and relatively small number of parameters (13,651 parameters for all cases above) independent of the cardinality q . In contrast, traditional embedding methods require significantly more parameters – linear in q – making MMembeddings substantially less prone to overfitting, especially for larger q . Additional experiments examining inclusion of multiple categorical features,

q	Metric	Ignore	Embed.	EmbedL2	REmbed.	UEmbed.	MMbed.
Regression							
10^2	MSE_Y	5.29 (.18)	3.67 (.11)	3.74 (.14)	5.25 (.17)	4.09 (.11)	3.46 (.11)
	$RMSE_D$	–	0.47 (.01)	0.50 (.01)	0.48 (.01)	0.47 (.01)	0.29 (.01)
	AUC_B	–	0.68 (.01)	0.65 (.02)	0.64 (.01)	0.66 (.02)	0.71 (.01)
10^3	MSE_Y	4.90 (.35)	3.98 (.28)	3.95 (.23)	4.82 (.36)	4.06 (.10)	3.36 (.20)
	$RMSE_D$	–	0.40 (.01)	0.43 (.01)	0.40 (.01)	0.41 (.01)	0.27 (.01)
	AUC_B	–	0.68 (.01)	0.63 (.02)	0.67 (.02)	0.67 (.01)	0.71 (.02)
10^4	MSE_Y	5.12 (.29)	3.42 (.12)	3.51 (.16)	3.92 (.17)	3.95 (.11)	3.01 (.09)
	$RMSE_D$	–	0.34 (.01)	0.37 (.01)	0.27 (.01)	0.36 (.01)	0.23 (.01)
	AUC_B	–	0.69 (.03)	0.62 (.04)	0.72 (.03)	0.69 (.01)	0.73 (.03)
10^5	MSE_Y	4.93 (.21)	3.60 (.11)	3.70 (.11)	3.50 (.10)	3.95 (.11)	3.10 (.09)
	$RMSE_D$	–	0.35 (.01)	0.38 (.01)	0.21 (.01)	0.34 (.01)	0.24 (.01)
	AUC_B	–	0.69 (.02)	0.58 (.02)	0.73 (.02)	0.70 (.01)	0.72 (.01)
Classification							
10^2	AUC_Y	0.67 (.01)	0.82 (.01)	0.80 (.01)	0.67 (.01)	0.78 (.01)	0.82 (.01)
	$RMSE_D$	–	0.48 (.01)	0.52 (.01)	0.49 (.01)	0.48 (.02)	0.33 (.01)
	AUC_B	–	0.66 (.02)	0.63 (.02)	0.67 (.02)	0.61 (.01)	0.72 (.01)
10^3	AUC_Y	0.71 (.01)	0.82 (.01)	0.81 (.01)	0.74 (.01)	0.78 (.00)	0.84 (.00)
	$RMSE_D$	–	0.40 (.01)	0.42 (.01)	0.37 (.01)	0.43 (.01)	0.26 (.01)
	AUC_B	–	0.62 (.01)	0.58 (.01)	0.65 (.01)	0.63 (.01)	0.65 (.01)
10^4	AUC_Y	0.71 (.01)	0.82 (.01)	0.82 (.01)	0.78 (.01)	0.79 (.01)	0.85 (.01)
	$RMSE_D$	–	0.36 (.00)	0.38 (.00)	0.31 (.01)	0.36 (.01)	0.24 (.00)
	AUC_B	–	0.65 (.01)	0.61 (.02)	0.68 (.01)	0.69 (.01)	0.69 (.01)
10^5	AUC_Y	0.71 (.01)	0.83 (.01)	0.71 (.01)	0.81 (.01)	0.79 (.01)	0.86 (.01)
	$RMSE_D$	–	0.35 (.01)	0.38 (.01)	0.27 (.01)	0.36 (.01)	0.25 (.01)
	AUC_B	–	0.67 (.02)	0.50 (.00)	0.70 (.02)	0.68 (.02)	0.71 (.02)

Table 1: Performance metrics across embedding methods on simulated datasets for regression and classification tasks with a single high-cardinality categorical feature of cardinality q . Mean test predictive performance (MSE_Y and AUC_Y), embedding quality ($RMSE_D$), and downstream embedding utility (AUC_B) are reported, with standard errors in parentheses. Bold indicates non-inferior to the best performance per row by a paired t-test.

and other variations in simulation parameters are detailed in Appendix D, including scatterplots of predicted versus true embeddings for each latent dimension (Figure 3).

To conclude this part, Figure 2 compares computational efficiency and generalization performance of MMembeddings with competing methods on the simulated regression data. The left panel shows mean runtime per epoch against increasing categorical cardinality q , with the sample size n set to $10q$. While MMembeddings scale similarly to alternative approaches, their computational overhead is higher compared to standard embeddings. The right panel illustrates validation loss over epochs for $q = 10^4$. Standard embeddings quickly exhibit severe overfitting, indicating that early stopping or additional regularization is essential. In contrast, MMembeddings substantially reduce overfitting while using roughly one-tenth of the embedding parameters.

4.2 Real data

We now present results for MMembeddings applied to real-world datasets. We demonstrate our method’s capabilities first on a substantial classification dataset within a collaborative filtering framework, and subsequently on several regression datasets characterized by high-cardinality categorical features.

Classification with Neural Collaborative Filtering We test MMembeddings within the neural collaborative filtering (NCF) framework [9, 26], using the Amazon video games ratings dataset [22]. The dataset originally consists of approximately 1.3 million tuples containing user IDs, video game IDs, ratings, and timestamps. We sampled 100K user-game interactions with ratings of 5, interpreting these as positive interactions. Following the implicit feedback methodology of [9], we consider these interactions as positive samples (labeled “1”) and additionally generate 100K negative samples (labeled “0”) by selecting user-game combinations not present in the original data. Timestamps for

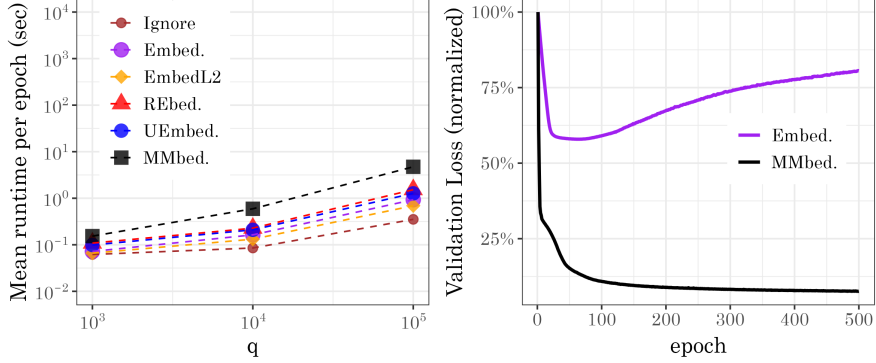


Figure 2: Left: Mean runtime per epoch (log-log scale) is shown for varying cardinality q (with sample size $n = 10q$), regression setting. Right: The validation loss plot (normalized) for $q = 10^4$.

		NCF-Embeddings (1.2M params)			NCF-MMbeddings (5.4K params)		
batch		$n_p = 2$	$n_p = 5$	$n_p = 10$	$n_p = 2$	$n_p = 5$	$n_p = 10$
AUC	10^3	.69 (.006)	.65 (.001)	.65 (.002)	.69 (.001)	.70 (.001)	.70 (.001)
	10^4	.68 (.004)	.66 (.006)	.65 (.003)	.70 (.001)	.70 (.001)	.71 (.001)
LogLoss	10^3	.84 (.021)	1.6 (.016)	2.2 (.016)	.64 (.000)	.64 (.001)	.64 (.001)
	10^4	.66 (.005)	.77 (.013)	1.0 (.028)	.64 (.002)	.64 (.002)	.64 (.001)
Accuracy	10^3	.64 (.004)	.60 (.002)	.60 (.001)	.65 (.001)	.65 (.001)	.65 (.001)
	10^4	.65 (.003)	.63 (.006)	.61 (.002)	.65 (.001)	.65 (.001)	.66 (.001)

Table 2: Performance of standard embeddings vs. MMembeddings in NCF on the Amazon video games ratings dataset, across varying batch sizes and patience epochs (n_p), with 10-CV standard errors in parentheses. MMembeddings' performance improvements (AUC, accuracy), and reductions (LogLoss), are statistically significant under a paired t-test.

negative samples were drawn from each user’s existing timestamp distribution. Hence, our task transforms into a challenging binary classification problem involving recommending items (games) to users, with additional temporal features. Our dataset thus comprises $n = 200K$ total samples, $p = 10$ continuous timestamp-based features, and two high-cardinality categorical features representing users ($q_{users} = 90K$) and games ($q_{games} = 20K$).

We implement the NCF architecture by embedding users and items into latent vectors, calculating their inner products, concatenating additional temporal features, and then applying a decoder to output probabilities using a sigmoid activation. Specifically, we compare standard embedding layers and UEmbeddings versus our MMembeddings method, integrating the variational loss component. For MMembeddings, we use a single-layer encoder of 100 neurons and ReLU activation, all variance priors were set to 0.5, and the variational hyperparameter β_V was fixed at 0.1. All models were trained using 10-fold cross-validation with a batch size varying in $\{10^3, 10^4\}$, an early stopping procedure with $n_p \in \{2, 5, 10\}$ epochs patience monitoring a 10% validation set, with a latent dimension $d = 10$ and the same decoder – a two-layer MLP with 10 neurons in each layer. UEmbeddings performed very poorly across multiple choices of q_U ; thus, we omit their results here. This outcome is understandable, as the inner product-based NCF architecture does not naturally align with the unified embedding framework of UEmbeddings.

Table 2 shows mean AUC, logloss, and accuracy on unseen data. MMembeddings consistently outperform standard embeddings with about two orders of magnitude fewer parameters (5.4K vs. 1.2M). While standard embeddings quickly overfit (increasing logloss as n_p grows), MMembeddings maintain stable or slightly improved performance, highlighting robustness in high-cardinality scenarios.

Regression with TabTransformer For regression, we evaluate MMembeddings on the five datasets from [29], each containing multiple high-cardinality categorical features (see Table 3 for a concise overview and Appendix E for more extensive descriptions). As an illustrative example, the UK Biobank (UKB) dataset [30] comprises 42K cancer patients with five high-cardinality categorical

Dataset	n, p	categorical (q)	y	Metric	TT-Em.	TT-UEm.	TT-MM.
Imdb	86K, 159	director (38K) movie type (2K)	movie ratings	MSE param	1.20 (.02) 407K	1.29 (.01) 19K	1.14 (.01) 29K
News	81K, 176	source (5.4K) title (72K)	item shares	MSE param	2.57 (.01) 790K	2.45 (.02) 90K	2.36 (.02) 11K
IE	73K, 3	student (2.9K) teacher (1.1K) department (14)	teacher ratings	MSE param	1.51 (.01) 48K	1.51 (.01) 88K	1.49 (.00) 13K
Spotify	28K, 14	artist (10K) album (22K) playlist (2.3K) subgenre (553)	song dance-ability	MSE param	.014 (.00) 368K	.012 (.00) 17K	.012 (.00) 17K
UKB	42K, 19	treatment (1.1K) operation (2.0K) diagnosis (2.1K) cancer type (446) histology (359)	triglyc. level	MSE param	0.99 (.02) 68K	0.95 (.01) 17K	0.94 (.01) 19K

Table 3: Performance of standard embeddings, UEmbeddings and MMembeddings in TabTransformer on [29]’s categorical regression datasets, with 10-CV standard errors in parentheses. Bold indicates non-inferior to the best performance per row by a paired t-test.

variables: diagnosis, operation, treatment, cancer type, and tumor histology. The task involves predicting standardized triglyceride levels in the blood (mmol/L).

We compare standard embeddings, UEmbeddings and MMembeddings using the TabTransformer architecture, effective for tabular data. MMembeddings employs a single-layer encoder (100 neurons, ReLU) outputting means and log-variances, with fixed $\beta_V = 0.1$ and variance priors at 0.1. All methods share latent dimension $d = 10$, early stopping (patience = 5 epochs, 10% validation), and an identical decoder (two layers, 10 neurons each) on the transformer output. Batch size is optimized per method and q_U for UEmbeddings.

Critically, although all methods share identical inference-time architectures, standard embeddings require substantially more parameters, proportional to each categorical cardinality q_k , resulting in 3-70 times greater complexity and potential overfitting. Table 3 summarizes results, demonstrating MMembeddings consistently achieve superior predictive performance with fewer parameters.

5 Conclusion

We introduced MMembeddings, a novel method that integrates random effects from NLMM into a VAE to model categorical embeddings. This approach reduces parameter complexity and mitigates overfitting in high-cardinality settings. Experiments on simulated and real data show that MMembeddings outperform traditional embeddings and other encoding methods in both accuracy and robustness.

Our method notably maintains a fixed and modest parameter count, independent of the categorical feature cardinality. This robustness becomes particularly pronounced as cardinality increases, positioning MMembeddings as a practical and theoretically grounded solution for modern predictive modeling challenges involving categorical data.

For future research, MMembeddings can naturally incorporate more complex, non-diagonal covariance structures when additional relational information, such as knowledge graphs between categorical levels, is available. Although our current diagonal covariance assumption simplifies computations and has empirically demonstrated strong performance, leveraging known relationships between categories – for instance, the number of shared movies between movie raters [36] – could further improve embedding quality and predictive capabilities.

Additionally, preliminary results indicate promising extensions of MMembeddings to sequence and text data, where embeddings typically take the form of three-dimensional tensors $(n_b, n_{\text{sequence}}, d)$. We have working code for such settings, demonstrating good initial performance, suggesting the potential broad applicability and scalability of our approach beyond tabular data.

Acknowledgments and Disclosure of Funding

This study was supported in part by a fellowship from the Edmond J. Safra Center for Bioinformatics at Tel-Aviv University, by Israel Science Foundation grant 2180/20 and by Israel Council for Higher Education Data-Science Centers.

References

- [1] Sercan Ö. Arik and Tomas Pfister. Tabnet: Attentive interpretable tabular learning. *Proceedings of the AAAI Conference on Artificial Intelligence*, 35(8):6679–6687, May 2021. doi: 10.1609/aaai.v35i8.16826. URL <https://ojs.aaai.org/index.php/AAAI/article/view/16826>.
- [2] Douglas Bates, Martin Mächler, Ben Bolker, and Steve Walker. Fitting linear mixed-effects models using lme4. *Journal of Statistical Software*, 67(1):1–48, 2015. doi: 10.18637/jss.v067.i01.
- [3] Hao Chen, Lili Zheng, Raed AL Kontar, and Garvesh Raskutti. Stochastic gradient descent in correlated settings: A study on gaussian processes. In H. Larochelle, M. Ranzato, R. Hadsell, M. F. Balcan, and H. Lin, editors, *Advances in Neural Information Processing Systems*, volume 33, pages 2722–2733. Curran Associates, Inc., 2020. URL <https://proceedings.neurips.cc/paper/2020/file/1cb524b5a3f3f82be4a7d954063c07e2-Paper.pdf>.
- [4] Benjamin Coleman, Wang-Cheng Kang, Matthew Fahrbach, Ruoxi Wang, Lichan Hong, Ed Chi, and Derek Cheng. Unified embedding: Battle-tested feature representations for web-scale ml systems. In A. Oh, T. Naumann, A. Globerson, K. Saenko, M. Hardt, and S. Levine, editors, *Advances in Neural Information Processing Systems*, volume 36, pages 56234–56255. Curran Associates, Inc., 2023. URL https://proceedings.neurips.cc/paper_files/paper/2023/file/afcac2e300bc243d15c25cd4f4040f0d-Paper-Conference.pdf.
- [5] Paul Covington, Jay Adams, and Emre Sargin. Deep neural networks for youtube recommendations. In *Proceedings of the 10th ACM Conference on Recommender Systems*, Rec-Sys ’16, page 191–198, New York, NY, USA, 2016. Association for Computing Machinery. ISBN 9781450340359. doi: 10.1145/2959100.2959190. URL <https://doi.org/10.1145/2959100.2959190>.
- [6] Cheng Guo and Felix Berkhahn. Entity embeddings of categorical variables, 2016.
- [7] Huirong Guo, Ruiming Tang, Yunming Ye, Zhenguo Li, and Xiuqiang He. Deepfm: A factorization-machine based neural network for ctr prediction, 2017. URL <https://arxiv.org/abs/1703.04247>.
- [8] John T. Hancock and Taghi M. Khoshgoftaar. Survey on categorical data for neural networks. *Journal of Big Data*, 7(1):28, Apr 2020. ISSN 2196-1115. doi: 10.1186/s40537-020-00305-w. URL <https://doi.org/10.1186/s40537-020-00305-w>.
- [9] Xiangnan He, Lizi Liao, Hanwang Zhang, Liqiang Nie, Xia Hu, and Tat-Seng Chua. Neural collaborative filtering. In *Proceedings of the 26th International Conference on World Wide Web*, WWW ’17, page 173–182, Republic and Canton of Geneva, CHE, 2017. International World Wide Web Conferences Steering Committee. ISBN 9781450349130. doi: 10.1145/3038912.3052569. URL <https://doi.org/10.1145/3038912.3052569>.
- [10] Irina Higgins, Loic Matthey, Arka Pal, Christopher Burgess, Xavier Glorot, Matthew Botvinick, Shakir Mohamed, and Alexander Lerchner. beta-VAE: Learning basic visual concepts with a constrained variational framework. In *International Conference on Learning Representations*, 2017. URL <https://openreview.net/forum?id=Sy2fzU9g1>.
- [11] Xin Huang, Ashish Khetan, Milan Cvitkovic, and Zohar Karnin. Tabtransformer: Tabular data modeling using contextual embeddings, 2020. URL <https://arxiv.org/abs/2012.06678>.
- [12] Diederik P Kingma and Max Welling. Auto-encoding variational bayes, 2013. URL <https://arxiv.org/abs/1312.6114>.
- [13] Max Kuhn and Kjell Johnson. *Feature engineering and selection: A practical approach for predictive models*. Chapman and Hall/CRC, 2019.
- [14] Marc Lavielle and Leon Aarons. What do we mean by identifiability in mixed effects models? *Journal of Pharmacokinetics and Pharmacodynamics*, 43(1):111–122, Feb 2016. ISSN 1573-8744. doi: 10.1007/s10928-015-9459-4. URL <https://doi.org/10.1007/s10928-015-9459-4>.

[15] Zixuan Liang. Efficient representations for high-cardinality categorical variables in machine learning, 2025. URL <https://arxiv.org/abs/2501.05646>.

[16] Yu-Wei Lin, Yuqian Zhou, Faraz Faghri, Michael J. Shaw, and Roy H. Campbell. Analysis and prediction of unplanned intensive care unit readmission using recurrent neural networks with long short-term memory. *PLoS ONE*, 14(7), July 2019. doi: 10.1371/journal.pone.0218942. URL <https://doi.org/10.1371/journal.pone.0218942>.

[17] Mary J. Lindstrom and Douglas M. Bates. Nonlinear mixed effects models for repeated measures data. *Biometrics*, 46(3):673–687, 1990. ISSN 0006341X, 15410420. URL <http://www.jstor.org/stable/2532087>.

[18] Charles E. McCulloch, Shayle R. Searle, and John M. Neuhaus. *Generalized, Linear, and Mixed Models*. John Wiley and Sons, Inc., June 2008. ISBN 978-0-470-07371-1.

[19] Tomas Mikolov, Kai Chen, Greg Corrado, and Jeffrey Dean. Efficient estimation of word representations in vector space, 2013. URL <https://arxiv.org/abs/1301.3781>.

[20] Thomas Mock. Tidy tuesday: A weekly data project aimed at the r ecosystem, 2022. URL <https://github.com/rfordatascience/tidytuesday>.

[21] Nuno Moniz and Luis Torgo. Multi-source social feedback of online news feeds. *CoRR*, 2018.

[22] Jianmo Ni, Jiacheng Li, and Julian McAuley. Justifying recommendations using distantly-labeled reviews and fine-grained aspects. In *Proceedings of the 2019 conference on empirical methods in natural language processing and the 9th international joint conference on natural language processing (EMNLP-IJCNLP)*, pages 188–197, 2019.

[23] Steffen Rendle. Factorization machines. In *2010 IEEE International Conference on Data Mining*, pages 995–1000, 2010. doi: 10.1109/ICDM.2010.127.

[24] Ronald Richman and Mario V. Wüthrich. High-cardinality categorical covariates in network regressions. *Japanese Journal of Statistics and Data Science*, 7(2):921–965, Nov 2024. ISSN 2520-8764. doi: 10.1007/s42081-024-00243-4. URL <https://doi.org/10.1007/s42081-024-00243-4>.

[25] Michal Rolinek, Dominik Zietlow, and Georg Martius. Variational autoencoders pursue pca directions (by accident), 2018. URL <https://arxiv.org/abs/1812.06775>.

[26] Badrul Sarwar, George Karypis, Joseph Konstan, and John Riedl. Item-based collaborative filtering recommendation algorithms. In *Proceedings of the 10th International Conference on World Wide Web*, WWW '01, page 285–295, New York, NY, USA, 2001. Association for Computing Machinery. ISBN 1581133480. doi: 10.1145/371920.372071. URL <https://doi.org/10.1145/371920.372071>.

[27] Hao-Jun Michael Shi, Dheevatsa Mudigere, Maxim Naumov, and Jiyan Yang. Compositional embeddings using complementary partitions for memory-efficient recommendation systems. In *Proceedings of the 26th ACM SIGKDD International Conference on Knowledge Discovery & Data Mining*, KDD '20, page 165–175, New York, NY, USA, 2020. Association for Computing Machinery. ISBN 9781450379984. doi: 10.1145/3394486.3403059. URL <https://doi.org/10.1145/3394486.3403059>.

[28] Giora Simchoni and Saharon Rosset. Using random effects to account for high-cardinality categorical features and repeated measures in deep neural networks. In M. Ranzato, A. Beygelzimer, Y. Dauphin, P.S. Liang, and J. Wortman Vaughan, editors, *Advances in Neural Information Processing Systems*, volume 34, pages 25111–25122. Curran Associates, Inc., 2021. URL <https://proceedings.neurips.cc/paper/2021/file/d35b05a832e2bb91f110d54e34e2da79-Paper.pdf>.

[29] Giora Simchoni and Saharon Rosset. Integrating random effects in deep neural networks. *Journal of Machine Learning Research*, 24(156):1–57, 2023. URL <http://jmlr.org/papers/v24/22-0501.html>.

[30] Cathie Sudlow, John Gallacher, Naomi Allen, Valerie Beral, Paul Burton, John Danesh, Paul Downey, Paul Elliott, Jane Green, Martin Landray, Bette Liu, Paul Matthews, Giok Ong, Jill Pell, Alan Silman, Alan Young, Tim Sprosen, Tim Peakman, and Rory Collins. Uk biobank: An open access resource for identifying the causes of a wide range of complex diseases of middle and old age. *PLOS Medicine*, 12(3):1–10, 03 2015. doi: 10.1371/journal.pmed.1001779. URL <https://doi.org/10.1371/journal.pmed.1001779>.

[31] Dan Tito Svenstrup, Jonas Hansen, and Ole Winther. Hash embeddings for efficient word representations. In I. Guyon, U. Von Luxburg, S. Bengio, H. Wallach, R. Fergus, S. Vishwanathan, and R. Garnett, editors, *Advances in Neural Information Processing Systems*, volume 30. Curran Associates, Inc., 2017. URL https://proceedings.neurips.cc/paper_files/paper/2017/file/f0f6ba4b5e0000340312d33c212c3ae8-Paper.pdf.

[32] Kilian Weinberger, Anirban Dasgupta, John Langford, Alex Smola, and Josh Attenberg. Feature hashing for large scale multitask learning. In *Proceedings of the 26th Annual International Conference on Machine Learning*, ICML ’09, page 1113–1120, New York, NY, USA, 2009. Association for Computing Machinery. ISBN 9781605585161. doi: 10.1145/1553374.1553516. URL <https://doi.org/10.1145/1553374.1553516>.

[33] Andrew G Wilson, Zhiting Hu, Russ R Salakhutdinov, and Eric P Xing. Stochastic variational deep kernel learning. In D. Lee, M. Sugiyama, U. Luxburg, I. Guyon, and R. Garnett, editors, *Advances in Neural Information Processing Systems*, volume 29. Curran Associates, Inc., 2016. URL <https://proceedings.neurips.cc/paper/2016/file/bcc0d400288793e8bcd7c19a8ac0c2b-Paper.pdf>.

[34] Andrew Gordon Wilson, Zhiting Hu, Ruslan Salakhutdinov, and Eric P. Xing. Deep kernel learning. In Arthur Gretton and Christian C. Robert, editors, *Proceedings of the 19th International Conference on Artificial Intelligence and Statistics*, volume 51 of *Proceedings of Machine Learning Research*, pages 370–378, Cadiz, Spain, 09–11 May 2016. PMLR. URL <https://proceedings.mlr.press/v51/wilson16.html>.

[35] Wrandler. Imdb new dataset, Jan 2021. URL <https://www.kaggle.com/datasets/wrandler/imdb-new-dataset>.

[36] Liwei Wu, Shuqing Li, Cho-Jui Hsieh, and James L Sharpenack. Stochastic shared embeddings: Data-driven regularization of embedding layers. In H. Wallach, H. Larochelle, A. Beygelzimer, F. d’Alché-Buc, E. Fox, and R. Garnett, editors, *Advances in Neural Information Processing Systems*, volume 32. Curran Associates, Inc., 2019. URL https://proceedings.neurips.cc/paper_files/paper/2019/file/37693cf748049e45d87b8c7d8b9aacd-Paper.pdf.

[37] Yunyang Xiong, Hyunwoo J. Kim, and Vikas Singh. Mixed effects neural networks (menets) with applications to gaze estimation. In *Proceedings of the IEEE/CVF Conference on Computer Vision and Pattern Recognition (CVPR)*, June 2019.

A Combining the means and variances for each cluster

In constructing the MMbeddings framework, a natural question arises regarding how best to aggregate encoder outputs for observations belonging to the same categorical level j within a minibatch ξ . Our current implementation computes the average of both the means $\boldsymbol{\mu}_i^\xi$ and the (log) variances $\log \left(\left[\boldsymbol{\tau}_i^\xi \right]^2 \right)$ across all observations assigned to level j . While this approach may seem like a straightforward design choice, it stems from a deeper analysis of the statistical structure underlying RE models.

To motivate this choice, consider the posterior distribution of a random intercept b_{0j} in a standard LMM:

$$y_{ij} = \mathbf{x}_{ij}^T \boldsymbol{\beta} + b_{0j} + \varepsilon_{ij}, \quad b_{0j} \sim \mathcal{N}(0, \sigma_b^2), \quad \varepsilon_{ij} \sim \mathcal{N}(0, \sigma^2).$$

The posterior mean of b_{0j} , given the n_j observations from cluster j , is well known to be a shrinkage estimator:

$$\mathbb{E}[b_{0j} | \mathbf{X}_j, \mathbf{y}_j] = \frac{\sigma_b^2}{\sigma^2/n_j + \sigma_b^2} (\bar{y}_j - \bar{\mathbf{x}}_j^T \boldsymbol{\beta}).$$

Assuming $\sigma^2 = \sigma_b^2$, this expression simplifies to

$$\frac{n_j}{n_j + 1} (\bar{y}_j - \bar{\mathbf{x}}_j^T \boldsymbol{\beta}).$$

This offers an intuitive interpretation: the posterior mean interpolates between the prior (zero) and the within-cluster residual mean. When $n_j = 1$, the shrinkage factor becomes $\frac{1}{2}$; as $n_j \rightarrow \infty$, it approaches 1, recovering the full residual mean.

Likewise, the posterior variance of b_{0j} is given by:

$$\text{Var}[b_{0j} \mid \mathbf{X}_j, \mathbf{y}_j] = \left(\frac{n_j}{\sigma^2} + \frac{1}{\sigma_b^2} \right)^{-1},$$

which simplifies under the same assumption to $\frac{\sigma^2}{n_j + 1}$, again shrinking to 0 as $n_j \rightarrow \infty$.

These classical results suggest that the degree of shrinkage – both in mean and variance – should depend on the number of observations per cluster. In our setting, however, the encoder does not explicitly account for the number of observations per categorical level when generating its outputs $\boldsymbol{\mu}_i$ and $\boldsymbol{\tau}_i$. This led us to explore whether applying a corrective shrinkage factor c_j to the averaged encoder outputs could improve performance. Specifically, we considered two strategies:

- **Heuristic shrinkage:** Multiplying the averaged outputs for cluster j by a fixed factor $c_j = \frac{n_{\xi,j}}{n_{\xi,j} + 1}$, mimicking the classical LMM expression.
- **Learned scaling:** Introducing a learnable parameter c_j for each cluster, trained via back-propagation.

Surprisingly, empirical comparisons on both simulated and real datasets revealed that the best-performing strategy was to use simple averaging with no additional scaling. This was somewhat unexpected, given that in many practical scenarios – including high-cardinality categorical data – the average minibatch contains at most one representative per level, i.e., $n_{\xi,j} \in \{0, 1\}$ for most j . The result might suggest that attempts to impose additional shrinkage introduce more noise than benefit when $n_{\xi,j}$ is small and unstable.

In summary, although richer schemes inspired by LMM theory are plausible and theoretically grounded, the naive averaging approach seems to provide an effective empirical solution across sparse and dense cluster regimes alike.

B Formula for the non-linear function used in simulated data

$$\begin{aligned} f(\mathbf{X}, \mathbf{B}) = & 0.1e^{-\beta_{1j}X_1^2} + \text{clip} \left(\frac{\beta_{2j}X_2}{1 + \beta_{3j}X_3^2}, -5, 5 \right) + \sin(\beta_{4j}X_4) + \beta_{5j}X_5 \\ & + \frac{\beta_{6j}X_6}{1 + e^{-\beta_{7j}X_7}} + \arctan(\beta_{8j}X_8) + \beta_{9j} \cos(X_9) + \beta_{10j} \log(1 + X_{10}^2), \end{aligned}$$

where $\beta_{mj} = \beta_m + B_{jm}$ for $m = 1, \dots, 10$, and $\beta_m = 1$ for all m .

C A formula for normalized RMSE between distance matrices

$$\text{RMSE}_D = \sqrt{\frac{\frac{1}{q(q-1)} \sum_{i < j} (D_{true}^{ij} - D_{est}^{ij})^2}{\max(D_{true}) - \min(D_{true})}},$$

where D_{true} and D_{est} are $q \times q$ distance matrices of the true and estimated embeddings, respectively.

D Simulated datasets additional results

	Ignore	Embed.	EmbedL2	REmbed.	UEmbed.	MMbed.
$\sigma_m^2 = 0.3$						
MSE_Y	1.71 (.04)	1.70 (.02)	1.57 (.02)	1.72 (.03)	1.73 (.02)	1.63 (.02)
$RMSE_D$	–	0.32 (.01)	0.38 (.00)	0.29 (.01)	0.33 (.02)	0.16 (.00)
AUC_B	–	0.61 (.02)	0.57 (.02)	0.63 (.02)	0.60 (.02)	0.65 (.02)
$\sigma_m^2 = 3.0$						
MSE_Y	8.84 (.59)	5.47 (.16)	5.99 (.24)	6.58 (.27)	7.11 (.21)	4.88 (.14)
$RMSE_D$	–	0.37 (.00)	0.39 (.00)	0.31 (.01)	0.39 (.01)	0.26 (.01)
AUC_B	–	0.64 (.02)	0.57 (.03)	0.65 (.02)	0.63 (.01)	0.65 (.02)

Table 4: Performance metrics across embedding methods on simulated datasets for regression with $q = 10^4$, under varying true priors. Bold indicates non-inferior to the best performance per row by a paired t-test.

q	Metric	$\sigma_m^2 = 0.1$	$\sigma_m^2 = 1.0$ (*)	$\sigma_m^2 = 2.0$	$d = 5$	$d = 10$ (*)	$d = 20$
10^3	MSE_Y	3.22 (.09)	3.34 (.07)	3.09 (.07)	3.22 (.09)	3.34 (.07)	3.21 (.08)
	$RMSE_D$	0.34 (.01)	0.26 (.01)	0.24 (.01)	0.27 (.01)	0.26 (.01)	0.25 (.01)
	AUC_B	0.70 (.02)	0.71 (.01)	0.71 (.02)	0.72 (.02)	0.71 (.01)	0.71 (.02)
10^4	MSE_Y	3.06 (.08)	2.95 (.07)	2.94 (.06)	3.21 (.09)	2.95 (.07)	3.03 (.08)
	$RMSE_D$	0.31 (.00)	0.24 (.00)	0.21 (.00)	0.25 (.00)	0.24 (.00)	0.22 (.00)
	AUC_B	0.69 (.01)	0.69 (.01)	0.71 (.02)	0.69 (.02)	0.69 (.01)	0.71 (.02)

Table 5: Performance of MMbeddings under incorrect hyperparameter specifications in simulated regression scenarios (true prior variance $\sigma_m^2 = 1$, true latent dimension $d = 10$). Mean predictive performance (MSE_Y), embedding quality ($RMSE_D$), and downstream embedding utility (AUC_B) are reported with standard errors in parentheses, varying either the prior variance or latent dimension. Interestingly, for $q = 10^3$, the true parameter values (*) do not yield optimal performance.

	LMMNN	TabNet(Embed.)	TabTrans.(Embed.)	FeatHash.	MeanEnc	MMbed.
Regression MSE_Y						
10^2	3.84 (.10)	4.99 (.11)	3.98 (.10)	3.60 (.12)	5.14 (.17)	3.46 (.11)
10^3	3.38 (.11)	5.02 (.24)	4.23 (.21)	4.20 (.28)	4.90 (.36)	3.36 (.20)
10^4	3.85 (.35)	5.32 (.31)	3.93 (.12)	4.97 (.28)	5.13 (.30)	3.01 (.09)
10^5	3.51 (.10)	4.42 (.16)	4.10 (.10)	4.94 (.20)	4.93 (.21)	3.10 (.09)
Classification AUC_Y						
10^2	0.82 (.01)	0.65 (.01)	0.80 (.01)	0.82 (.01)	0.70 (.01)	0.82 (.01)
10^3	0.82 (.02)	0.67 (.01)	0.80 (.01)	0.79 (.00)	0.71 (.01)	0.84 (.00)
10^4	0.81 (.02)	0.67 (.00)	0.80 (.01)	0.72 (.00)	0.71 (.01)	0.85 (.01)
10^5	0.83 (.01)	0.78 (.01)	0.81 (.01)	0.71 (.01)	0.71 (.01)	0.86 (.01)

Table 6: Performance metrics for more architectures and encodings in addition to Table 1 on simulated datasets for regression and classification tasks with a single high-cardinality categorical feature of cardinality q . Mean test predictive performance (MSE_Y and AUC_Y) are reported, with standard errors in parentheses. Bold indicates non-inferior to the best performance per row by a paired t-test.

Method	Regression			
	MSE_Y	$RMSE_D$	AUC_D	n_{params}
MMbed.	11.19 (.21)	0.28 (.00)	0.57 (.01)	17891
Embed.	12.32 (.27)	0.36 (.00)	0.59 (.01)	300531
EmbedL2	11.47 (.25)	0.37 (.00)	0.59 (.01)	300531
REmbd.	12.24 (.31)	0.32 (.00)	0.60 (.01)	600531
UEmbd.	12.36 (.27)	–	–	10486291
FeatHash.	13.28 (.36)	–	–	30951
LMMNN	11.91 (.19)	–	–	235
TabNet	19.46 (.59)	–	–	339779
TabTrans.	20.52 (.39)	–	–	306829
MeanEnc	12.88 (.38)	–	–	531
Ignore	12.82 (.39)	–	–	231
Method	Classification			
	AUC_Y	$RMSE_D$	AUC_D	n_{params}
MMbed.	0.82 (.00)	0.28 (.00)	0.55 (.01)	17891
Embed.	0.80 (.00)	0.36 (.00)	0.59 (0.01)	300531
EmbedL2	0.81 (.00)	0.37 (.00)	0.50 (.00)	300531
REmbd.	0.79 (.00)	0.36 (.00)	0.60 (0.01)	600531
UEmbd.	0.80 (.00)	–	–	10486291
FeatHash.	0.79 (.00)	–	–	30951
LMMNN	–	–	–	–
TabNet	0.74 (.01)	–	–	339779
TabTrans.	0.68 (.01)	–	–	306829
MeanEnc	0.80 (.00)	–	–	531
Ignore	0.80 (.00)	–	–	231

Table 7: Performance metrics on simulated datasets with three high-cardinality categorical features of cardinality $[10^4, 10^4, 10^4]$ and $n = 100K$. The same architecture as in the single feature experiment is used, with a batch size of 10^4 . Mean test predictive performance (MSE_Y), embedding quality ($RMSE_D$), and downstream embedding utility (AUC_B) are reported, with standard errors in parentheses. Bold indicates non-inferior to the best performance per row by a paired t-test. Notice LMMNN cannot currently fit multiple categorical features for classification.

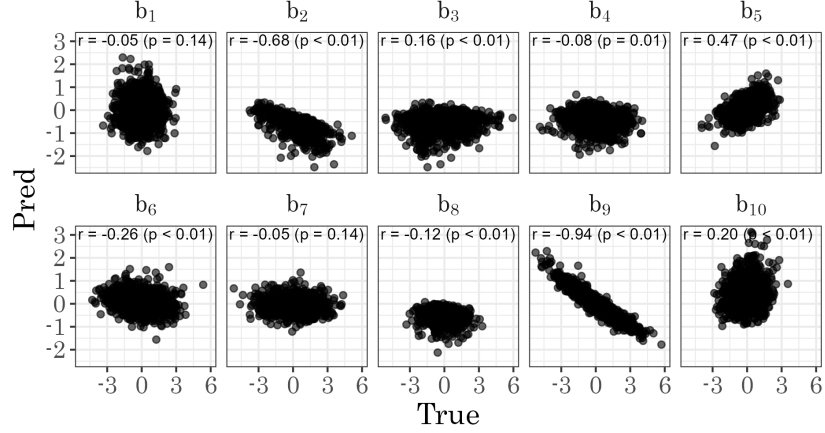


Figure 3: Predicted vs. true embedding values for each component b_1 to b_{10} , for the $q = 10^3$ cardinality scenario, regression setting. For each true component (\mathbf{B}), the most correlated predicted component (column in $\hat{\mathbf{B}}$) was selected based on Pearson correlation. Axis limits are shared across facets to ensure comparability.

E Real datasets additional details

Dataset	Source	Availability	Reference	Description
Imdb	Kaggle	Free	Wrangler [35]	86K movie titles scraped from imdb.com along with their genre, director, date of release a 1-10 mean score and a textual description which is processed to top 1-gram tokens count.
News	UCI ML	Free	Moniz and Torgo [21]	81K news items and their number of shares on Facebook. Headline is processed to top 1-gram tokens count.
InstEval	lme4	Free	Bates et al. [2]	73K students 1-5 evaluations of professors from ETH Zurich
Spotify	Tidy Tuesday	Free	Mock [20]	28K songs with their date release, genre, artist, album as well as 12 audio features from which we chose to predict the first one, danceability.
UKB-blood	UK Biobank	Authorized	Sudlow et al. [30]	Subset of 42K UK Biobank with cancer history. To predict triglycerides and other chemicals level in blood we use features such as gender, age, height, weight, skin color and more.

Table 8: Real datasets from [29]: additional details and references.